

## FULL PAPER

# Synthesis, characterization, density functional theory studies and antibacterial activity of a new Schiff base dioxomolybdenum(VI) complex with tryptophan as epoxidation catalyst

Zeinab Asgharpour<sup>1</sup> | Faezeh Farzaneh<sup>1</sup>  | Mina Ghiasi<sup>1</sup> | Mohammad Azarkish<sup>2</sup>

<sup>1</sup>Department of Chemistry, Faculty of Physics and Chemistry, Alzahra University, PO Box 1993891176, Vanak, Tehran, Iran

<sup>2</sup>Department of Chemistry, Payame Noor University (PNU), 19395-4697 Tehran, Iran

**Correspondence**

Faezeh Farzaneh, Department of Chemistry, Faculty of Physics and Chemistry, Alzahra University, PO Box 1993891176, Vanak, Tehran, Iran.

Email: faezeh\_farzaneh@yahoo.com; Farzaneh@alzahra.ac.ir

A *cis*-dioxomolybdenum(VI) complex was prepared with MoO<sub>2</sub>(acac)<sub>2</sub> and a Schiff base ligand (2-((2-hydroxybenzylidene)amino)-3-(1*H*-indol-3-yl)propanoic acid) derived from salicylaldehyde and L-tryptophan in ethanol and designated as [MoO<sub>2</sub>(Sal-Tryp)(EtOH)]. It was characterized using several techniques including thermogravimetric and elemental analyses and mass, Fourier transform infrared and UV–visible spectroscopies. Theoretical calculations were performed using density functional theory for studying the molecular structure. An *in vitro* antibacterial activity evaluation showed that [MoO<sub>2</sub>(Sal-Tryp)EtOH] complex exhibits good inhibitory effects against Gram-positive (*Bacillus subtilis*, *Staphylococcus aureus*) and Gram-negative (*Escherichia coli*, *Pseudomonas aeruginosa*) bacteria in comparison to standard antibacterial drugs. It was also found that [MoO<sub>2</sub>(Sal-Tryp)EtOH] complex successfully catalyses the epoxidation of cyclooctene, norbornene, cyclohexene, styrene,  $\alpha$ -methylstyrene and *trans*-stilbene, with 45–100% conversions and 64–100% selectivities. Based on the obtained results, the heterogeneity and reusability of the catalyst seem promising.

**KEYWORDS**

amino acid Schiff base ligand, antibacterial activity, dioxomolybdenum(VI) complex, epoxidation catalyst

## 1 | INTRODUCTION

Molybdenum is an essential metal that is less toxic than many other metals of industrial importance. The coordination chemistry of molybdenum(VI) has attracted considerable attention due to the enzymatic role of molybdenum in reduction reactions of molecular nitrogen and nitrate in plants and hydroxylation of xanthine and aldehydes in animals.<sup>[1,2]</sup>

The ability of molybdenum to form stable complexes with oxygen-, nitrogen- and sulfur-containing ligands led to development of molybdenum Schiff base complexes.<sup>[3]</sup> Molybdenum dioxo Schiff base complexes are excellent enzyme model systems for the active sites of transferase enzymes like nitrate reductase, the active sites of which consist of a *cis*-MoO<sub>2</sub> moiety.<sup>[4,5]</sup> In addition to the application

of molybdenum(VI) Schiff base complexes possessing Mo=O in electrochemistry,<sup>[6]</sup> particular attention has been paid to applications such as antibacterial<sup>[7,8]</sup> and antitumour<sup>[9]</sup> agents, olefin epoxidation catalysts,<sup>[10–12]</sup> sulfide oxidation,<sup>[13,14]</sup> hydrogen generation<sup>[15]</sup> and oxidation of benzyl alcohols.<sup>[16]</sup> Schiff base complexes derived from amino acids have attracted much attention because of their inorganic and biological importance.<sup>[17–19]</sup> Schiff base complexes derived from salicylaldehyde or 2-hydroxynaphthaldehyde with amino acids can be used as non-enzymatic models analogous to intermediates in metabolic reactions of amino acids such as transamination, racemization, decarboxylation and  $\alpha$ - or  $\beta$ -elimination.<sup>[20,21]</sup>

The epoxidation of alkenes is one of the most widely studied reactions in organic chemistry, since epoxides are

key starting materials for forming a wide variety of products such as alcohols, polyethers and aldehydes which have widespread application in the chemical and pharmaceutical industries, and in epoxy resins, epoxy paints, surfactants, pesticides, agrochemicals, perfume materials and sweeteners.<sup>[22,23]</sup> The type of ligand structure present in the complex and the catalytic reaction conditions have a significant effect on the catalytic activity of complexes involving the Mo(VI) metal centre.<sup>[24]</sup> As a result, several research groups have focused on the design of new dioxo Mo(VI) complexes and investigation of their catalytic behaviour as epoxidation catalysts.<sup>[25–37]</sup>

In many cases, density functional theory (DFT) calculations have been used in understanding the molecular properties of compounds, providing good assignment of experimental spectra and illustration of reaction mechanisms.<sup>[38]</sup>

In the study reported here, attempts were made to synthesize a new amino acid Schiff base complex of Mo with tryptophan and salicylaldehyde. Details of DFT studies in order to compare theoretical and experimental results together with an investigation of epoxidation catalytic behaviour and antibacterial activity of the complex are described in this paper.

## 2 | EXPERIMENTAL

### 2.1 | Materials and methods

All materials were of commercial reagent grade and used without further purification. *t*-Butyl hydroperoxide (TBHP; 70% in H<sub>2</sub>O) and cyclooctene were purchased from Fluka and Sigma-Aldrich, respectively. Salicylaldehyde, L-tryptophan, sodium acetate, norbornene, cyclohexene, styrene,  $\alpha$ -methylstyrene, *trans*-stilbene, acetonitrile, ethanol, chloroform, dichloromethane and carbon tetrachloride were purchased from Merck.

Fourier transform infrared (FT-IR) spectra were recorded with a Bruker Tensor 27 FT-IR spectrometer using KBr pellets over the range 400–4000 cm<sup>-1</sup>. Elemental analyses were performed with a Heraeus CHN-O-Rapid elemental analyser. UV–visible spectral measurements were performed with a double-beam PerkinElmer Lambda 35 spectrophotometer. The <sup>1</sup>H NMR spectrum was recorded in DMSO-*d*<sub>6</sub> with a Bruker DPX spectrometer. Chemical analyses of samples were determined with a PerkinElmer atomic absorption spectrometer. Thermogravimetric analysis (TGA) was carried out with a PerkinElmer Pyris Diamond TG/DTA, with a nitrogen atmosphere, the flow rate and heating rate being 80 mg min<sup>-1</sup> and 10 °C min<sup>-1</sup>, respectively. The mass spectrum of the complex was obtained with an HP (Agilent Technologies) 5937 Mass Selective Detector. Oxidation products were analysed using GC and GC-MS with an Agilent 6890 Series with a flame ionization detector, HP-5, 5%

phenylmethylsiloxane capillary and an Agilent 5973 Network, mass selective detector, HP-5 MS 6989 Network GC system.

### 2.2 | Synthesis of [MoO<sub>2</sub>(Sal-Tryp)(EtOH)]

Salicylaldehyde (0.1 ml, 1 mmol, in 2 ml of ethanol) was introduced into a tryptophan solution (204 mg, 1 mmol, in 2 ml of water). Upon addition of an aqueous sodium acetate solution (164 mg, 2 mmol, in 1 ml of water), the colour changed to yellow. Then, MoO<sub>2</sub>(acac)<sub>2</sub><sup>[39]</sup> solution (247 mg, 1 mmol, in 10 ml of ethanol) was prepared and added to the mixture followed by heating at reflux for 3 h while stirring. The white resultant solid was filtered, washed with water, ethanol and diethyl ether, and dried in air at room temperature. Yield 70%; decomposition point 288–290°C. Anal. Calcd for C<sub>20</sub>H<sub>20</sub>MoN<sub>2</sub>O<sub>6</sub> (*M* = 480.32 g mol<sup>-1</sup>) (%): Mo, 19.97; C, 50.01; H, 4.20; N, 5.83. Found (%): Mo, 20.14; C, 50.63; H, 3.98; N, 6.11. FT-IR (KBr pellet, cm<sup>-1</sup>): 1658 (C=N), 1557, 1307 (COO), 896, 871 (*cis*-MoO<sub>2</sub>), 513 (Mo–O), 422 (Mo–N).<sup>[40,41]</sup> UV–visible (DMSO,  $\lambda_{\max}$ , nm): 275 ( $\epsilon = 22\,500\text{ M}^{-1}\text{ cm}^{-1}$ ), 283 ( $\epsilon = 24\,000\text{ M}^{-1}\text{ cm}^{-1}$ ), 290 ( $\epsilon = 21\,167\text{ M}^{-1}\text{ cm}^{-1}$ ).<sup>[42,43]</sup> <sup>1</sup>H NMR (250 MHz, DMSO-*d*<sub>6</sub>,  $\delta$ , ppm): 1.70 (3H, CH<sub>3</sub>), 2.49–2.96 (2H, CH<sub>2</sub>), 3.26–3.43 (4H, CH<sub>2</sub>, CH, OH), 6.92–7.55 (9H, Ar), 10.92 (1H, NH).

### 2.3 | General procedure for oxidation of alkenes

To a mixture of catalyst (0.020 g) in CCl<sub>4</sub> (5 ml) was added the desired alkene (10 mmol) and TBHP (12 mmol, 1.6 ml) in a round-bottom flask. The suspension was then heated at reflux for 8 h. After filtration and washing the catalyst with CCl<sub>4</sub>, the solution was subjected to GC and GC–MS.

### 2.4 | *Ab Initio* molecular orbital calculation

All calculations were performed using Gaussian 98 software.<sup>[44]</sup> The geometries of the ligand and complex were fully optimized using the Hartree–Fock density functional scheme, the adiabatic connection method, Becke three-parameter with Lee–Yang–Parr (B3LYP) functional of DFT<sup>[45]</sup> with the standard 6-311G\*\* basis set. Restricted formalism was applied to all closed-shell systems. Full optimizations were performed without any symmetry constraints. Harmonic vibrational frequencies were computed to confirm that an optimized geometry correctly corresponded to a local minimum that had only real frequencies. The solvent effects on the conformational equilibrium and contribution to the total enthalpies were investigated with the PCM method<sup>[46]</sup> at the B3LYP/6-31G\*\* level. Tomasi's polarized continuum model defines the cavity as the union of a series of

interlocking atomic spheres. The effect of polarization of the solvent continuum was represented numerically. Solvation calculations were carried out for ethanol with the geometry optimization for this solvent. NMR computations of absolute shieldings were performed using the GIAO method for the DFT optimized structure in the presence of solvent. The  $^1\text{H}$  chemical shifts were calculated by using the corresponding absolute shielding calculated for  $\text{Me}_4\text{Si}$  at the same level of theory for both ligand and complex in DMSO as solvent.

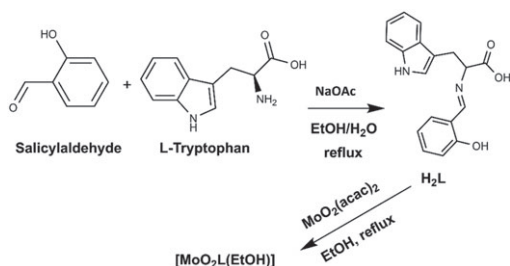
### 3 | RESULTS AND DISCUSSION

#### 3.1 | Characterization of $[\text{MoO}_2(\text{Sal-Tryp})(\text{EtOH})]$ complex

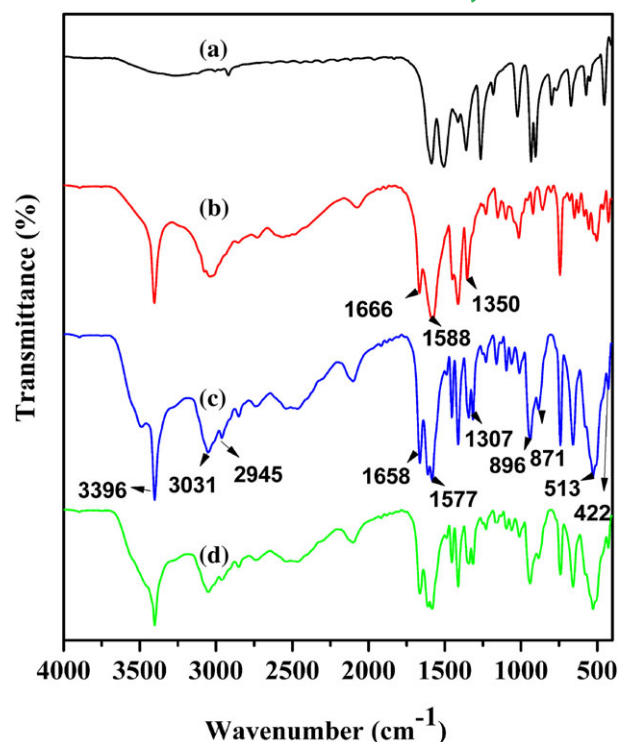
Salicylaldehyde and L-tryptophan were treated with  $\text{MoO}_2(\text{acac})_2$  in ethanol and water. As seen in Scheme 1, the initially generated *N*-salicylidene-L-tryptophan Schiff base ligand undergoes complexation with  $\text{MoO}_2(\text{acac})_2$  affording  $[\text{MoO}_2(\text{Sal-Tryp})(\text{EtOH})]$ .

MS was used to determine the molecular ion mass as well as molecular fragments to confirm the proposed structure of  $[\text{MoO}_2(\text{Sal-Tryp})(\text{EtOH})]$  complex. This method is particularly useful when a poorly crystalline nature of a complex prevents its X-ray crystallography characterization.<sup>[47,48]</sup> The mass spectrum of the complex shown in Figure S1 (supporting information) shows  $m/z$  480 corresponding to the complex  $\text{M}^+ + 1$ . The fragments appearing at  $m/z$  309 (base peak) and 204 are attributed to Schiff base and L-tryptophan ions, generated from parent  $\text{M}^+ + 1$  followed by sequential loss of  $[\text{MoO}_2(\text{EtOH})]$  and  $[\text{C}_9\text{H}_{11}\text{MoO}_4]$  radicals. Therefore, the proposed complex structure of  $[\text{MoO}_2(\text{Sal-Tryp})(\text{EtOH})]$  is confirmed.

The FT-IR spectra of  $\text{MoO}_2(\text{acac})$ , (Sal-Tryp) Schiff base ligand and  $[\text{MoO}_2(\text{Sal-Tryp})(\text{EtOH})]$  before and after reaction are shown in Figure 1, respectively. The bands appearing at 1658, 1577 and  $1307\text{ cm}^{-1}$  (Figure 1a, b, c, d)<sup>[49]</sup> are due to the  $\text{C}=\text{N}$  and  $\text{COO}^-$  asymmetric and symmetric stretching of Schiff base ligand coordinated to the metal. The rather large difference between asymmetric and symmetric  $\text{COO}^-$  frequencies indicates a monodentate coordination of this group. Two bands at 896 and  $871\text{ cm}^{-1}$  regions are due to the  $\text{Mo}=\text{O}$  vibrations (Figure 1b).  $\text{Mo}-\text{O}$  and  $\text{Mo}-\text{N}$



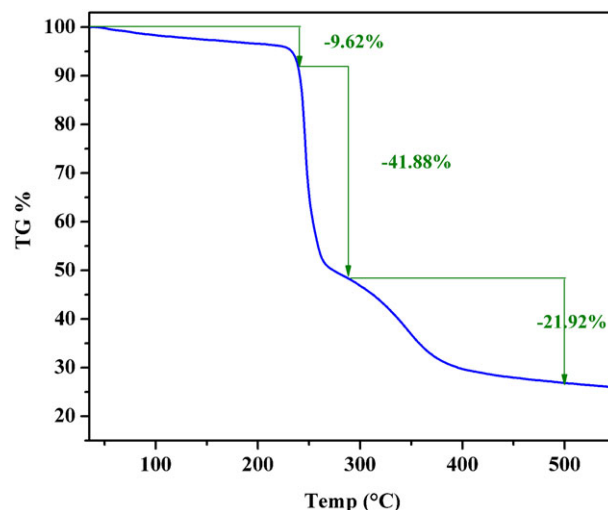
**SCHEME 1** Preparation of  $[\text{MoO}_2(\text{Sal-Tryp})(\text{EtOH})]$  complex



**FIGURE 1** FT-IR spectra: (a)  $\text{MoO}_2(\text{acac})_2$ ; (b) Sal-tryp Schiff base ligand;  $[\text{MoO}_2(\text{Sal-tryp})(\text{EtOH})]$  complex (c) before and (d) and after epoxidation

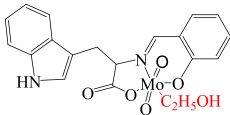
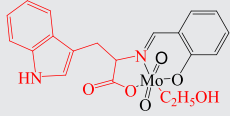
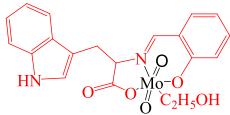
stretching bands generated by coordination of O and N atoms to Mo appear at 513 and  $424\text{ cm}^{-1}$ , respectively.<sup>[50]</sup>

To evaluate the thermal stability, the thermal decomposition of  $[\text{MoO}_2(\text{Sal-Tryp})(\text{EtOH})]$  complex was studied (Figure 2; Table 1). TGA carried out from 25 up to  $500\text{ }^\circ\text{C}$  indicates that  $[\text{MoO}_2(\text{Sal-Tryp})(\text{EtOH})]$  complex decomposes in three steps. The first step occurring at  $30\text{--}130\text{ }^\circ\text{C}$  corresponds to the liberation of solvent molecule (obs. 9.62%; calc. 9.59%). The second stage appears in the range



**FIGURE 2** TGA curve of  $[\text{MoO}_2(\text{Sal-Tryp})(\text{EtOH})]$  complex

**TABLE 1** TGA results for complex decomposition

Entry	Complex fragments	Removed fragment	Calc.	Obs.
1		EtOH	9.59	9.62
2		C <sub>11</sub> H <sub>10</sub> N <sub>2</sub> O <sub>2</sub>	41.91	41.88
3		C <sub>7</sub> H <sub>5</sub> O	21.89	21.92

150–247 °C, representing the decomposition of organic compounds as well as solvent removing (obs. 41.88%; calc. 41.99%). The last step observed in the range 250–400 °C (obs. 21.92%; calc. 21.89%) indicates the decomposition of the remaining organic compounds with the formation of molybdenum oxide. Finally above 500 °C, the weight of the remaining complex remains constant.

The electronic absorption spectrum of the complex in DMF exhibits three absorption bands at 275, 283 and 290 nm due to the benzene  $\pi \rightarrow \pi^*$ , imine  $\pi \rightarrow \pi^*$  and  $n \rightarrow \pi^*$  transitions of Schiff base of azomethine.<sup>[42,51]</sup>

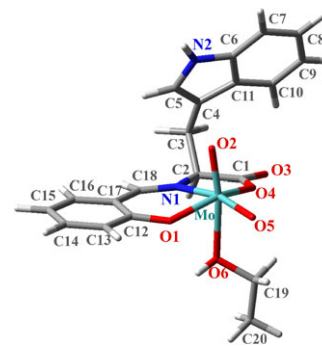
## 3.2 | Theoretical

### 3.2.1 | Geometry optimization of (Sal-Tryp) Schiff base ligand

The structure of the (Sal-Tryp) Schiff base ligand was fully optimized with the B3LYP method using 6-311G\*\* basis set, with no initial symmetry restrictions and assuming C<sub>1</sub> point group. The optimized geometries of the (Sal-Tryp) Schiff base ligand in the gas phase were re-optimized by considering the solvent effect using the PCM method. The optimized geometry of the ligand and some structural details are depicted in Figure S4 and given in Table S1, respectively.

### 3.2.2 | Geometry optimization of [MoO<sub>2</sub>(Sal-Tryp)(EtOH)] complex

In the next step, the fully optimized geometries of [MoO<sub>2</sub>(Sal-Tryp)(EtOH)] complex in gas phase were re-optimized by considering the solvent effect using PCM method (Figure 3 and Table S2). The calculated results

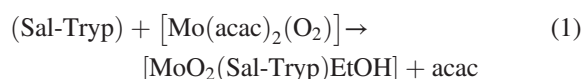
**FIGURE 3** Optimized structure of [MoO<sub>2</sub>(Sal-Tryp)(EtOH)] complex in solvent

indicate that the complex is stabilized by 45.17 kcal mol<sup>-1</sup> in ethanol solvent, perhaps due to the high dipole moment of the complex (11.88 D).

The calculated net charges on [MoO<sub>2</sub>(Sal-Tryp)(EtOH)] complex are presented in Table S3. These partial charges are derived from natural bond orbital calculations. The net negative charge on O<sub>1</sub> (−0.644), O<sub>3</sub> (−0.478), O<sub>4</sub> (−0.559), O<sub>5</sub> (−0.383), O<sub>6</sub> (−0.522), N<sub>1</sub> (−0.585) and N<sub>2</sub> (−0.807) atoms in (Sal-Tryp) molecule is more than that on other atoms. The net charge on Mo is 1.116 when (Sal-Tryp) is coordinated. Significantly, whereas the calculated electron density on the donor oxygen and nitrogen atoms is less than expected, it is more than expected on the central ion. Thus, the net charge results confirm an electron transfer from the donor atoms of the (Sal-Tryp) ligand to the central Mo ion. <sup>1</sup>H NMR and <sup>13</sup>C NMR spectra of [MoO<sub>2</sub>(Sal-Tryp)(EtOH)] complex and (Sal-Tryp) Schiff base were measured in DMSO-*d*<sub>6</sub> and are shown in Figures S2 and S3, respectively (supporting information).

### 3.2.3 | Molecular orbital analysis

The model [MoO<sub>2</sub>(Sal-Tryp)EtOH] complex used in this study was generated when one optimized (Sal-Tryp) molecule come close to optimized [MoO<sub>2</sub>(acac)<sub>2</sub>] complex<sup>[26]</sup> in EtOH solvent:



To determine the nature of the bonds in [MoO<sub>2</sub>(Sal-Tryp)EtOH] complex, molecular orbital analysis was employed since this method is useful for presenting the factors influencing the stability of this complex. The highest occupied molecular orbital (HOMO) and lowest unoccupied molecular orbital (LUMO) of [MoO<sub>2</sub>(Sal-Tryp)EtOH] complex are

shown in Figure 4. The energy gap or  $E_{\text{HOMO}} - E_{\text{LUMO}}$ , an important stability index in characterizing the chemical reactivity and kinetic stability of a molecule,<sup>[51–53]</sup> is 0.11 au.

Moreover, the  $^1\text{H}$  NMR chemical shifts obtained for  $[\text{MoO}_2(\text{Sal-Tryp})\text{EtOH}]$  complex via calculation<sup>[54]</sup> have been compared to those obtained experimentally (Table S4, supporting information).

### 3.3 | Catalytic studies

Cyclooctene was used for our early exploration of epoxidation under the catalytic effect of  $[\text{MoO}_2(\text{Sal-Tryp})\text{EtOH}]$  complex. To determine the optimum reaction conditions, various parameters such as amount of catalyst, reaction time and effect of solvent were studied (Figures 5–7). As seen in Figure 5, increasing the amount of catalyst from 3 to 20 mg increases the conversion from 25 to 100% with 100% selectivity. Therefore, all epoxidation reactions were carried out using 20 mg of catalyst.

In the next step, it was found that increasing the reaction time from 1 to 8 h using 20 mg of catalyst increases the cyclooctene conversion from 10 to 100% with 100% selectivity (Figure 6).

Compared to solvents such as EtOH,  $\text{CH}_3\text{CN}$  and ethyl acetate which are totally inefficient for epoxidation reaction,  $\text{CHCl}_3$ ,  $\text{CH}_2\text{Cl}_2$  and  $\text{CCl}_4$  were found to be suitable solvents in the presence of 20 mg Schiff base complex within 8 h (Figure 7). The inefficiency of EtOH,  $\text{CH}_3\text{CN}$  and ethyl acetate may be rationalized by hard–soft acid base theory. Coordination of these solvents to hard Mo(VI) ion via hard O and N atoms retards reaction perhaps by inhibiting the coordination of TBHP to the metal centre. On the other hand, non-coordinative chlorinated solvents such as  $\text{CCl}_4$ ,  $\text{CHCl}_3$  and  $\text{CH}_2\text{Cl}_2$  make more efficient the coordination of TBHP to Mo(VI) ion followed by oxygen transfer to alkene. Obtaining 47 and 100% conversions respectively in  $\text{CH}_2\text{Cl}_2$  and  $\text{CCl}_4$

with the most (1.6 D) and least (0 D) dipole moments is consistent with a rather non-polar transition state.<sup>[55]</sup>

To test the generality of the method, epoxidation of a range of alkenes such as cyclooctene, norbornene, *trans*-stilbene, styrene and  $\alpha$ -methyl styrene was investigated under optimized reaction conditions (Table 2). Whereas cyclooctene exclusively gives the corresponding epoxide (Table 2, entry 1), cyclohexene undergoes allylic oxidation

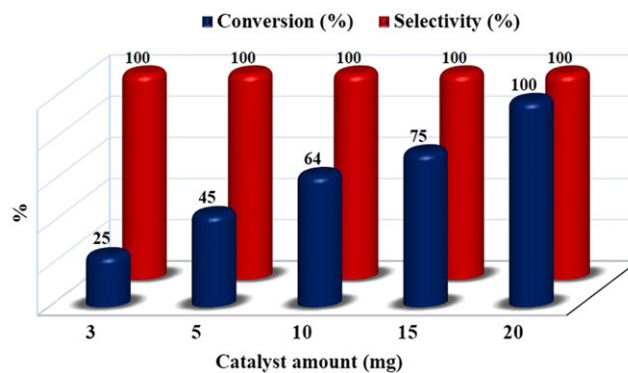


**FIGURE 5** Effect of amount of catalyst on the epoxidation of cyclooctene. Reaction conditions: cyclooctene (10 mmol), TBHP (14 mmol), solvent ( $\text{CCl}_4$ , 5 ml), under reflux condition, 8 h

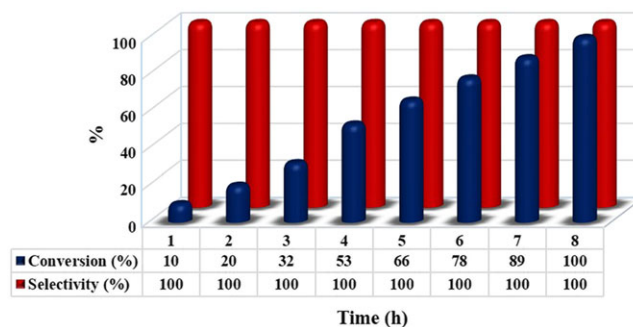


**FIGURE 6** Effect of time on epoxidation of cyclooctene. Reaction conditions: cyclooctene (10 mmol), TBHP (14 mmol), solvent ( $\text{CCl}_4$ , 5 ml), under reflux condition

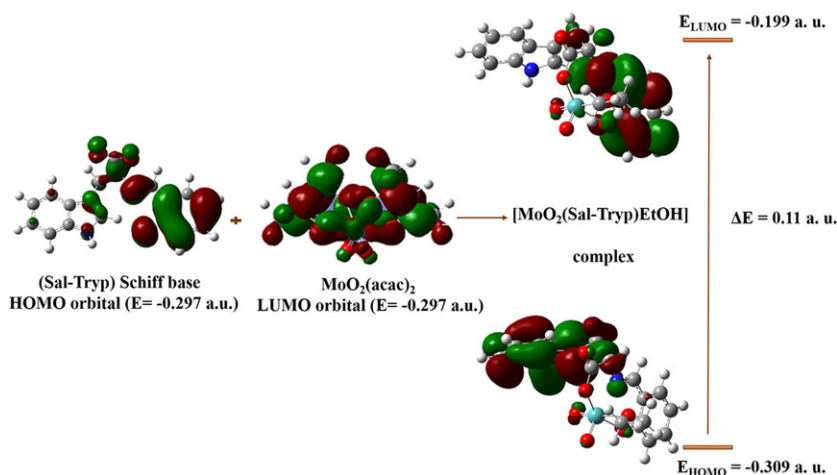


**FIGURE 4** Generation of  $[\text{MoO}_2(\text{Sal-Tryp})(\text{EtOH})]$  complex with HOMO and LUMO views of complex

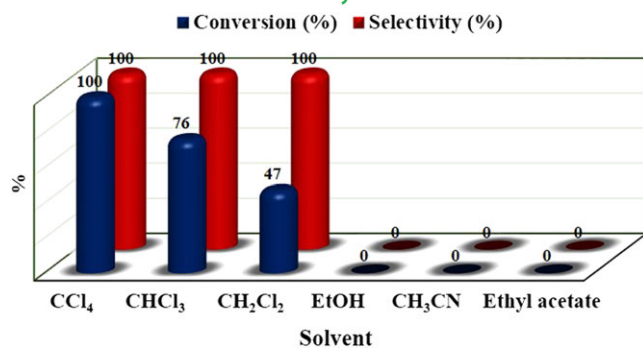


**FIGURE 7** Effect of solvent on catalytic epoxidation of cyclooctene. Reaction conditions: catalyst (20 mg), cyclooctene (10 mmol), TBHP (14 mmol), solvent (5 ml), reflux condition, 8 h

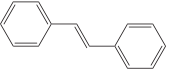
and epoxidation, concomitantly (Table 2, entry 3). It has been reported that the high epoxidation selectivity typically observed for cyclooctene is related to a poor  $\sigma_{C-\alpha H}-\pi_{C=C}$  orbital overlap in the predominant conformation (Scheme 2a). Therefore, such poor overlap disfavors the  $\alpha$ -H abstraction by radical species.<sup>[56]</sup> As such, allylic-site oxidation of cyclooctene is not in competition with epoxidation. On the other hand, cyclohexene exists in the half-

chair conformation in which allylic carbons lie in the plane of the double bond (Scheme 2b).<sup>[57]</sup> Therefore,  $\alpha$ -H abstraction by radical species competes with epoxidation, leading to 2-cyclohexene-1-ol/2-cyclohexene-1-one and cyclohexene epoxide, respectively.

Particularly significant is norbornene which selectively affords the corresponding epoxide (Table 2, entry 2). If norbornene undergoes allylic-site oxidation through  $\alpha$ -H abstraction by radical species, it affords a bridgehead radical which has been shown to be unstable due to Bredt's rule.<sup>[58]</sup> Therefore, norbornene conclusively undergoes epoxidation reaction, affording the corresponding epoxide. In the case of styrene, *trans*-stilbene and  $\alpha$ -methylstyrene, epoxidation is partly accompanied by generation of benzaldehyde, benzoic acid and acetophenone (Table 2, entries 4, 5 and 6). A further nucleophilic attack of TBHP on the styrene, stilbene and  $\alpha$ -methylstyrene oxides seems to be responsible for the formation of benzaldehyde and acetophenone. Benzaldehyde in turn is readily oxidized to benzoic acid.

The recyclability of [MoO<sub>2</sub>(Sal-Tryp)EtOH] complex as catalyst was investigated under optimum reaction conditions. After each reaction cycle with cyclooctene, the catalyst was recovered by centrifugation, washed three times with CCl<sub>4</sub> and dried under vacuum. It was found that after using the

**TABLE 2** Results obtained for epoxidation of different alkenes in the presence of Schiff base complex

Entry	Substrate	Conversion <sup>a</sup> (%)	Selectivity to epoxide (%)	TON <sup>b</sup>	TOF <sup>c</sup> (h <sup>-1</sup> )
1	 Cyclooctene	100	100	244	30.48
2	 Norbornene	78	100	190	23.78
3	 Cyclohexene	50	64 <sup>d</sup>	122	15.24
4	 Styrene	45	70 <sup>e</sup>	110	13.71
5	 <i>trans</i> -Stilbene	85	78 <sup>f</sup>	21	2.59
6	 $\alpha$ -methylstyrene	72	93 <sup>g</sup>	177	21.95

<sup>a</sup>Reaction conditions: catalyst (20 mg), substrate (alkenes (10 mmol), *trans*-stilbene (1 mmol)), TBHP (14 mmol), solvent (CCl<sub>4</sub>, 5 ml, reflux condition), time (8 h).

<sup>b</sup>TON: mmol of epoxide to the mmol molybdenum present in catalyst.

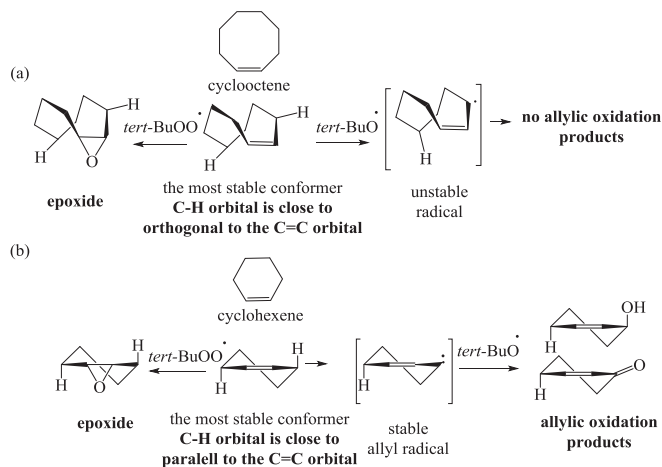
<sup>c</sup>TOF: turnover frequency which is calculated by the expression [epoxide]/[catalyst] × time (h<sup>-1</sup>).

<sup>d</sup>2-Cyclohexene-1-ol and 2-cyclohexene-1-one identified as byproduct.

<sup>e</sup>Benzaldehyde and benzoic acid identified as byproduct.

<sup>f</sup>Benzaldehyde and benzoic acid identified as byproduct.

<sup>g</sup>Acetophenone identified as byproduct.



**SCHEME 2** Suggested mechanism for oxidation of (a) cyclooctene and (b) cyclohexene

catalyst for five runs, there was a decrease in conversion from 100 to 94% without any changes in selectivity (Figure 8).

Since no catalytic activity is observed when the filtrate of each run is subjected to epoxidation conditions in the absence of the catalyst, it can be concluded that the catalyst is truly functioning heterogeneously. The Mo content in the catalyst before and after use in reaction is 20.14 and 20.12%, respectively. No significant desorption is observed during the course of reaction.

The XRD patterns of the complex before and after use as a catalyst are shown in Figure 9. The similarity in XRD patterns is evidence for the stability and heterogeneous character of the catalyst.

Finally, results of epoxidation of cyclooctene catalysed by  $[\text{MoO}_2(\text{Sal-Tryp})(\text{EtOH})]$  in the present study have been compared to those recently reported for some Mo catalytic epoxidations (Table 3). As is evident, results obtained for cyclooctene in the current work are comparable or even better in some cases.

### 3.4 | Antibacterial activity

The *in vitro* antibacterial activity of the prepared  $[\text{MoO}_2(\text{Sal-Tryp})(\text{EtOH})]$  complex was studied and compared with the

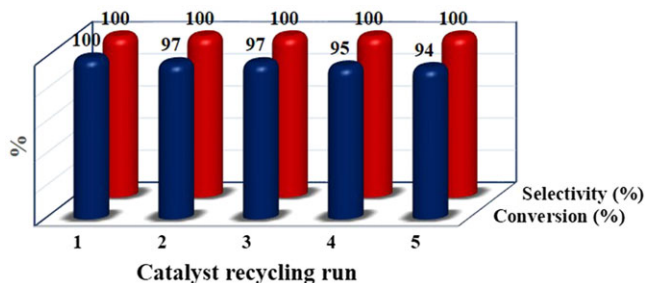


**FIGURE 8** Effect of recycling of  $[\text{MoO}_2(\text{Sal-Tryp})(\text{EtOH})]$  complex as catalyst in epoxidation of cyclooctene. Reaction conditions: catalyst (20 mg), cyclooctene (10 mmol), TBHP (14 mmol), solvent ( $\text{CCl}_4$ , 5 ml), reflux condition, 8 h

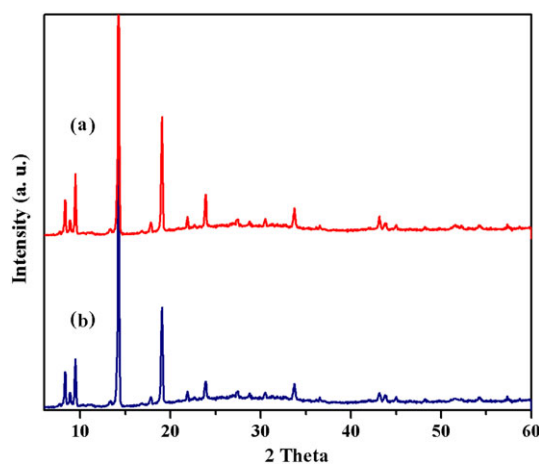


**FIGURE 9** XRD patterns of  $[\text{MoO}_2(\text{Sal-Tryp})(\text{EtOH})]$  complex (a) before and (b) after epoxidation reaction

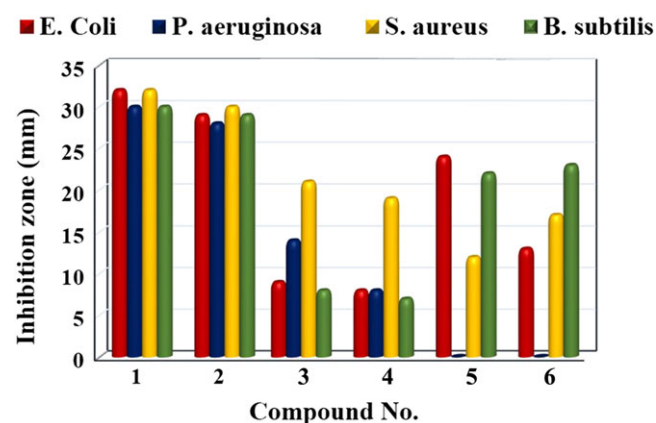
activity of two standard antibacterial drugs: nalidixic acid and vancomycin. The microorganisms used in this study were *Bacillus subtilis* and *Staphylococcus aureus* (as Gram-positive bacteria) and *Escherichia coli* and *Pseudomonas aeruginosa* (as Gram-negative bacteria). The tests were done at compound concentrations of 15 and 25  $\text{mg ml}^{-1}$ . As evident from Table 4 and shown in Figure 10, the complex at 15  $\text{mg ml}^{-1}$  exhibits good activity against *B. subtilis*, *S. aureus*, *E. coli* and *P. aeruginosa*. With increasing complex concentration to 25  $\text{mg ml}^{-1}$ , the inhibition effect of the complex increases against *B. subtilis* and leads to increasing inhibition zone for *E. coli*, *P. aeruginosa* and *S. aureus*. The antibacterial activity effect of the complex may be rationalized by chelation of ligand with metal. Partial sharing of ligand donor groups with the positive charge of the metal ion increases the delocalization of electrons over the whole ligand, which reduces the polarity of the metal ion and increases the lipophilic character of the central metal ion. The lipophilic character of the central metal ion favours

**TABLE 3** Comparison of epoxidation of cyclooctene catalysed by [MoO<sub>2</sub>(Sal-Tryp)EtOH] complex with some previously reported epoxidations catalysed by Mo compounds with TBHP

Entry	Catalyst	Conversion (%)	Selectivity (%)	TOF(h <sup>-1</sup> )	Ref.
1	[MoO <sub>2</sub> (Sal-Tryp)EtOH]	100	100	30.48	This work
2	Mo <sub>2</sub> Ar/ZAPS-PVPA	99	>99	6.25	[59]
3	MCM-41-SB-MoO <sub>2</sub> (acac)	94	100	14.7	[60]
4	[Mo(O) <sub>2</sub> (salen)-POM]	100	100	8.33	[61]
5	MoO <sub>2</sub> salen-SBA-15	49.1	49.1	25.6	[62]
6	Supported bis-acetylacetonatodioxo molybdenum complex on boehmite nanoparticles functionalized with imidazole	97	97	126	[63]
7	Supported bis-acetylacetonatodioxo molybdenum complex on boehmite nanoparticles functionalized with amine	97	97	89	[63]
8	MCM-41-supported molybdenum/bisdithiocarbamate	96	97	184	[64]
9	MoL <sub>1</sub>	100	100	100	[65]
10	MoO <sub>2</sub> alaacacAmpMCM-41	87	99	124	[66]
11	MoO <sub>2</sub> valacacAmpMCM-41	35	99	66	[66]

**TABLE 4** Quantitative antimicrobial assay results (zone of growth inhibition) of metal salt and [MoO<sub>2</sub>(Sal-Tryp)(EtOH)] complex

Compound	Concentration (mg ml <sup>-1</sup> )	Inhibition zone (mm)			
		<i>E. coli</i> (-)	<i>P. aeruginosa</i> (-)	<i>S. aureus</i> (+)	<i>B. subtilis</i> (+)
[MoO <sub>2</sub> (Sal-Tryp)(EtOH)]	25	32	30	32	30
	15	29	28	30	29
MoO <sub>2</sub> (acac) <sub>2</sub>	25	9	14	21	8
	15	8	8	19	7
Nalidixic acid	25	24	n.a.	12	22
Vancomycin	25	13	n.a.	17	23

**FIGURE 10** Antibacterial activities of (1) [MoO<sub>2</sub>(Sal-Tryp)(EtOH)] (25 mg ml<sup>-1</sup>), (2) [MoO<sub>2</sub>(Sal-Tryp)(EtOH)] (15 mg ml<sup>-1</sup>), (3) MoO<sub>2</sub>(acac)<sub>2</sub> (25 mg ml<sup>-1</sup>), (4) MoO<sub>2</sub>(acac)<sub>2</sub> (15 mg ml<sup>-1</sup>), (5) nalidixic acid standard (25 mg ml<sup>-1</sup>) and (6) vancomycin standard (25 mg ml<sup>-1</sup>)

permeation through the lipid layer of cell membranes and deactivating cellular enzymes that play important role in the metabolic pathways of microorganisms.<sup>[67–69]</sup> It is significant that the complex has good inhibition activity against *P. aeruginosa* while standard drugs show no activity against it. Also, the complex has greater antibacterial activity against *B. subtilis*, *S. aureus* and *E. coli* than the standard drugs.

## 4 | CONCLUSIONS

In this study, [MoO<sub>2</sub>(Sal-Tryp)EtOH] complex was prepared using MoO<sub>2</sub>(acac)<sub>2</sub> and (Sal-Tryp) Schiff base ligand. The molecular structure was determined with FT-IR, UV-visible and mass spectroscopies and TGA. The optimized geometric parameters (bond lengths and bond angles) were theoretically determined. The complex was used as a catalyst for the epoxidation of several olefins with TBHP with high conversion

yields and selectivities. The reusability of the catalyst was studied to evaluate its practical potential. Finally, the antibacterial activity of the [MoO<sub>2</sub>(Sal-Tryp)EtOH] complex against Gram-positive and Gram-negative bacteria in comparison to standard nalidixic acid and vancomycin antibiotics was evaluated.

## ACKNOWLEDGEMENT

The financial support from Alzakra University is gratefully acknowledged.

## REFERENCES

- [1] R. Hille, *J. Inorg. Chem.* **2006**, *10*, 1913.
- [2] S. Metz, W. Thiel, *J. Am. Chem. Soc.* **2009**, *131*, 14885.
- [3] C. J. Doonan, H. L. Wilson, K. Rajagopalan, R. M. Garrett, B. Bennett, R. C. Prince, G. N. George, *J. Am. Chem. Soc.* **2007**, *129*, 9421.
- [4] B. K. Burgess, D. J. Lowe, *Chem. Rev.* **1996**, *96*, 2983.
- [5] R. Hille, *Chem. Rev.* **1996**, *96*, 2757.
- [6] S. Alghool, C. Slebodnick, *Polyhedron* **2014**, *67*, 11.
- [7] H. A. Rudbari, M. Khorshidifard, B. Askari, N. Habibi, G. Bruno, *Polyhedron* **2015**, *100*, 180.
- [8] A. A. A. Aziz, *J. Mol. Struct.* **2010**, *979*, 77.
- [9] M. A. Hussein, T. S. Guan, R. A. Haque, M. B. K. Ahamed, A. M. A. Majid, *Polyhedron* **2015**, *85*, 93.
- [10] K. Ambroziak, R. Pelech, E. Milchert, T. Dziembowska, Z. Rozwadowski, *J. Mol. Catal. A* **2004**, *211*, 9.
- [11] M. Mohammadikish, M. Masteri-Farahani, S. Mahdavi, *J. Magn. Mater.* **2014**, *354*, 317.
- [12] J. Zhang, P. Jiang, Y. Shen, W. Zhang, X. Li, *Micropor. Mesopor. Mater.* **2015**, *206*, 161.
- [13] I. Sheikhshoae, A. Rezaeifard, N. Monadi, S. Kaafi, *Polyhedron* **2009**, *28*, 733.
- [14] S. Menati, H. A. Rudbari, M. Khorshidifard, F. Jalilian, *J. Mol. Struct.* **2016**, *1103*, 94.
- [15] J.-P. Cao, L.-L. Zhou, L.-Z. Fu, J.-X. Zhao, H.-X. Lu, S.-Z. Zhan, *Catal. Commun.* **2014**, *57*, 1.
- [16] B. Gao, M. Wan, J. Men, Y. Zhang, *Appl. Catal. A* **2012**, *439*, 156.
- [17] K. Serbest, A. Özen, Y. Ünver, M. Er, I. Değirmencioglu, K. Sancak, *J. Mol. Struct.* **2009**, *922*, 1.
- [18] A. Stanila, A. Marcu, D. Rusu, M. Rusu, L. David, *J. Mol. Struct.* **2007**, *834*, 364.
- [19] Y. Özcan, S. İde, L. F. Şakıyan, E. Logoglu, *J. Mol. Struct.* **2003**, *658*, 207.
- [20] P. Pyykkö, *Chem. Rev.* **1997**, *97*, 597.
- [21] B. M. Guirard, E. E. Snell, in *Comprehensive Biochemistry*, (Eds: M. Florkin, E. H. Stotz), Elsevier, Amsterdam **1981**.
- [22] A. K. Yudin, J. B. Sweeney, *Aziridines and Epoxides in Organic Synthesis*, Wiley-VCH Weinheim **2006**.
- [23] G. Sienel, R. Rieth, K. T. Rowbottom, *Ullmann's Encyclopedia of Industrial Chemistry*, Wiley-VCH, Weinheim **2000**.
- [24] K. Gupta, A. K. Sutar, *Coord. Chem. Rev.* **2008**, *252*, 1420.
- [25] S. Acharya, T. A. Hanna, *Polyhedron* **2016**, *107*, 113.
- [26] Z. Asgharpour, F. Farzaneh, A. Abbasi, M. Ghiasi, *Polyhedron* **2015**, *101*, 282.
- [27] P. Traar, J. A. Schachner, B. Stanje, F. Belaj, N. C. Mösch-Zanetti, *J. Mol. Catal. A* **2014**, *385*, 54.
- [28] W. Wang, T. Guerrero, S. R. Merecias, H. García-Ortega, R. Santillan, J.-C. Daran, N. Farfán, D. Agustin, R. Poli, *Inorg. Chim. Acta* **2015**, *431*, 176.
- [29] M. Bagherzadeh, M. Zare, M. Amini, T. Salemnoush, S. Akbayrak, S. Özkar, *J. Mol. Catal. A* **2014**, *395*, 470.
- [30] A. Rezaeifard, I. Sheikhshoae, N. Monadi, M. Alipour, *Polyhedron* **2010**, *29*, 2703.
- [31] C. Bibal, J.-C. Daran, S. Deroover, R. Poli, *Polyhedron* **2010**, *29*, 639.
- [32] Y. Sui, X. Zeng, X. Fang, X. Fu, Y. A. Xiao, L. Chen, M. Li, S. Cheng, *J. Mol. Catal. A* **2007**, *270*, 61.
- [33] L. Meng, Q. Cheng, C. Kim, W.-Y. Gao, L. Wojtas, Y.-S. Chen, M. J. Zaworotko, X. P. Zhang, S. Ma, *Angew. Chem. Int. Ed.* **2012**, *51*, 1.
- [34] W. Zhanga, P. Jianga, Y. Wanga, J. Zhangb, P. Zhangaa, *Appl. Catal. A* **2015**, *489*, 117.
- [35] W. Zhang, P. Jiang, Y. Wang, J. Zhang, Y. Gao, P. Zhang, *RSC Adv.* **2014**, *4*, 51544.
- [36] W. Zhang, W. Gao, T. Pham, P. Jiang, S. Ma, *Cryst. Growth Des.* **2016**, *16*, 1005.
- [37] W. Zhang, Y. Wang, Y. Leng, P. Zhang, J. Zhang, P. Jiang, *Catal. Sci. Technol.* **2016**, *6*, 5848.
- [38] E. Schott, X. Zarate, D. MacLeod-Carey, R. Arratia-Perez, C. Bustos, *Polyhedron* **2013**, *61*, 27.
- [39] G. J. Chen, J. W. McDonald, W. Newton, *Inorg. Chem.* **1976**, *15*, 2612.
- [40] L. Casella, M. Gullotti, A. Pintar, S. Colonna, A. Manfredi, *Inorg. Chim. Acta* **1988**, *144*, 89.
- [41] J. C. Pessoa, I. Cavaco, I. Correia, M. Duarte, R. Gillard, R. Henriques, F. Higes, C. Madeira, I. Tomaz, *Inorg. Chim. Acta* **1999**, *293*, 1.
- [42] P. Gürkan, N. Sari, *Synth. React. Inorg. Met.-Org. Chem.* **1999**, *29*, 753.
- [43] S. Y. Ebrahimipour, H. Khabazadeh, J. Castro, I. Sheikhshoae, A. Crochet, K. M. Fromm, *Inorg. Chim. Acta* **2015**, *427*, 52.
- [44] M. J. Frisch, G. W. Trucks, H. B. Schlegel, G. E. Scuseria, M. A. Robb, J. R. Cheeseman, V. G. Zakrzewski, J. A. Montgomery, R. E. Stratmann, J. C. Burant, S. Dapprich, J. M. Millam, A. D. Daniels, K. N. Kudin, M. C. Strain, O. Farkas, J. Tomasi, V. Barone, M. Cossi, R. Cammi, B. Mennucci, C. Pomelli, C. Adamo, S. Clifford, J. Ochterski, G. A. Petersson, P. Y. Ayala, Q. Cui, K. Morokuma, D. K. Malick, A. D. Rabuck, K. Raghavachari, J. B. Foresman, J. Cioslowski, J. V. Ortiz, B. B. Stefanov, G. Liu, A. Liashenko, P. Piskorz, I. Komaromi, R. Gomperts, R. L. Martin, D. J. Fox, T. Keith, M. A. Al-Laham, C. Y. Peng, A. Nanayakkara, C. Gonzalez, M. Challacombe, P. M. W. Gill, B. G. Johnson, W. Chen, M. W. Wong, J. L. Andres, M. Head-Gordon, E. S. Replogle, J. A. Pople, *Gaussian 98 (Revision A.1)*, Gaussian Inc., Pittsburgh, PA **1998**.

- [45] A. D. Becke, *J. Chem. Phys.* **1993**, *98*, 5648.
- [46] R. G. Parr, R. G. P. W. Yang, *Density-Functional Theory of Atoms and Molecules*, Oxford University Press, Oxford **1989**.
- [47] J. Sanmartin, F. Novio, A. M. Garcia-Deibe, M. Fondo, N. Ocampo, M. R. Bermejo, *Polyhedron* **2006**, *25*, 1714.
- [48] I. Beloso, J. Castro, J. A. Garcia-Vazquez, P. Perez-Lourido, J. Romero, A. Sousa, *Polyhedron* **2003**, *22*, 1099.
- [49] O. Rajan, A. Chakravorty, *Inorg. Chem.* **1981**, *20*, 660.
- [50] G. Wang, J. C. Chang, *Synth. React. Inorg. Met.* **1994**, *24*, 1091.
- [51] N. S. Rao, M. N. Jaiswal, D. D. Mishra, R. C. Maurya, N. Nageswara Rao, *Polyhedron* **1993**, *12*, 2045.
- [52] N. M. Hosny, M. A. Hussien, F. M. Radwan, N. Nawar, *Spectrochim. Acta A* **2014**, *132*, 121.
- [53] M. Govindarajan, S. Periandy, K. Carthigayen, *Spectrochim. Acta* **2012**, *97*, 411.
- [54] K. Wolinski, J. F. Hilton, P. Pulay, *J. Am. Chem. Soc.* **1990**, *112*, 8251.
- [55] T. H. Lowry, K. S. Richardson, *Mechanism and Theory in Organic Chemistry*, 3rd ed., Harper & Row, New York **1987**.
- [56] U. Neuenschwander, I. Hermans, *J. Org. Chem.* **2011**, *76*, 10236.
- [57] E. L. Eliel, S. H. Wilen, *Stereochemistry of Organic Compounds*, John Wiley, New York **1994**.
- [58] J. March, *Advanced Organic Chemistry*, 3rd ed., John Wiley, New York **1985**, 616.
- [59] Z. Hu, X. F. Y. Li, *Inorg. Chem. Commun.* **2011**, *14*, 497.
- [60] S. Tangestaninejad, M. Moghadam, V. Mirkhani, I. Mohammadpoor-Baltork, K. Ghani, *Catal. Commun.* **2009**, *10*, 853.
- [61] M. Moghadam, V. Mirkhani, S. Tangestaninejad, I. Mohammadpoor-Baltork, M. Moshref Javadi, *Polyhedron* **2010**, *29*, 648.
- [62] Y. Yanga, S. Hao, Y. Zhang, Q. Kana, *Solid State Sci.* **2011**, *13*, 1938.
- [63] M. Mirzaee, B. Bahramian, J. Gholizadeh, A. Feizi, R. Gholami, *Chem. Eng. J.* **2017**, *308*, 160.
- [64] F. Bigia, C. Giancarlo Piscopo, G. Predieria, G. Sartori, R. Scotti, R. Zanon, R. Maggi, *J. Mol. Catal. A* **2014**, *386*, 108.
- [65] S. Rayati, P. Abdolalian, *Appl. Catal. A* **2013**, *456*, 240.
- [66] M. Masteri-Farahani, *J. Mol. Catal. A* **2010**, *316*, 45.
- [67] A. Chaudhary, N. Bansal, A. Gajraj, R. V. Singh, *J. Inorg. Biochem.* **2003**, *96*, 393.
- [68] A. Kulkarni, P. G. Avaji, G. B. Bagihalli, P. S. Badami, S. A. Patil, *J. Coord. Chem.* **2009**, *62*, 481.
- [69] M. Maghami, F. Farzaneh, J. Simpson, M. Ghiasi, M. Azarkish, *J. Mol. Struct.* **2015**, *1093*, 24.

## SUPPORTING INFORMATION

Additional Supporting Information may be found online in the supporting information tab for this article.

**How to cite this article:** Asgharpour Z, Farzaneh F, Ghiasi M, Azarkish M. Synthesis, characterization, density functional theory studies and antibacterial activity of a new Schiff base dioxomolybdenum(VI) complex with tryptophan as epoxidation catalyst. *Appl Organometal Chem.* 2017;e3782. <https://doi.org/10.1002/aoc.3782>